

# Determination of inclination of strut and shear strength using variable angle truss model for shear-critical RC beams

Bing Li<sup>1\*</sup> and Cao Thanh Ngoc Tran<sup>2a</sup>

<sup>1</sup>School of Civil and Environment Engineering, Nanyang Technological University, 639798, Singapore

<sup>2</sup>Department of Civil Engineering, International University, Vietnam National University, Ho Chi Minh City, Vietnam

(Received September 7, 2010, Revised July 20, 2011, Accepted January 28, 2012)

**Abstract.** This paper attempts to determine the inclination of the compression strut within variable angle truss models for RC beams loaded in shear-flexure through a proposed semi-analytical approach. A truss unit is used to analyze a reinforced concrete beam, by the principle of virtual work under the truss analogy. The inclination of the compression strut is then theoretically derived. The concrete contribution is addressed by utilizing the compatibility condition within each truss unit. Comparisons are made between the predicted and published experimental results of the seventy one RC beams with respect to the shear strength and the inclined angle of the compression strut at this state to investigate the adequacy of the proposed semi-analytical approach.

**Keywords:** inclination of strut; truss model; concrete contribution; shear strength

---

## 1. Introduction

The truss analogy has been widely used as the basis of most shear design procedures for reinforced concrete (RC) beams (Collins *et al.* 1991, Ramirez *et al.* 1991, Li and Tran 2008, Wong and Kuang 2011). The inclined compression struts of the truss are assumed to represent the concrete stress blocks between adjacent cracks at the failure stage as shown in Fig. 1. The compression struts transfer external loads in the transverse direction to the tension ties. These tension ties provide the shear resistance in this truss analogy. The top and bottom chords of the truss consist of concrete stress blocks and longitudinal reinforcement, respectively. The chords are assumed to not contribute to the shear capacity of RC beams.

According to the aforesaid classical truss analogy, shear reinforcement ratio and inclination of compression strut  $\theta$  are two key quantities directly related to obtaining the shear capacity of RC beams. For simplicity, Ritter *et al.* (1899) and Morsch *et al.* (1902) assumed the compression struts to be inclined at  $45^\circ$  corresponding to the first shear cracking angle. The ACI 318 code adopted this

---

\*Corresponding author, Associate Professor, E-mail: [cbli@ntu.edu.sg](mailto:cbli@ntu.edu.sg)

<sup>a</sup>Lecturer, E-mail: [tctngoc@hcmiu.edu.vn](mailto:tctngoc@hcmiu.edu.vn)

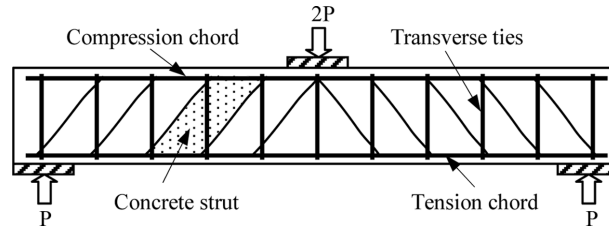


Fig. 1 Truss analogy for cracked beams subjected to shear and flexure

assumption. However, this assumption may lead to an underestimation of the contribution from the shear reinforcement, especially when the shear strength of lightly reinforced concrete beams are required to be determined. Consequently, Ramirez and Breen (1991) and Priestley *et al.* (1994) suggested taking  $30^\circ$  as the strut inclination. This approach uses a constant strut angle over the entire shear span of beams. However, all empirical results indicate that cracks form at variable orientations and at different regions of a beam, indicating the varying directions for diagonal compression. Hence, a variable angle of inclination would be more realistic. On this basis, variable angle truss models have been conceptually developed by Regan *et al.* (1969). However, quantification of the variable strut inclinations through mathematical or mechanical approaches has not been explicitly determined by these conceptual models. Also, little has been said about how these variable angle truss models can be related to a design process.

In the ACI 318 code (2008), the stirrup contribution is determined through a rational approach. The concrete contribution represents the difference between the stirrup contribution and the shear strength. A similar approach is taken by some other codes, in which, most of the concrete contribution terms are achieved through regression analysis of data from tested beams. A mechanical model considering some influential factors would provide a proper means to represent model codes for the shear carried by concrete.

Kim and Mander (1999) proposed a differential variable angle truss model in order to develop a comprehensive theory for modeling inelastic shear and flexural behavior. The model estimates the stiffness of a diagonally cracked short column in which the disturbed region prevailed. Numerical integration schemes were introduced to find the stiffness solution and then implemented on a truss model to determine the positions of the transverse ties and the dimensions of the compression struts. Decoupled shear and flexural analysis was performed on a few variable angle truss models to determine the deflection response and inclination of struts. Concrete tensile members were used to represent the concrete contribution to strength. Kim and Mander (1999) provided a valuable mathematical methodology to deal with the variable angle truss model of short columns. However, their formulations and solutions are limited to the disturbed region of short columns. By applying Kim and Mander (1999)'s method, the authors propose a rational approach to compute the inclination of compression struts in a variable angle truss model for shear-critical RC beams subjected to shear and flexure.

## 2. Inclination of strut in variable angle truss model

Fig. 2 shows the shear transfer mechanism for a typical region along a beam member. This transfer mechanism can be reasonably represented by the truss analogy as shown in Fig. 3. Under

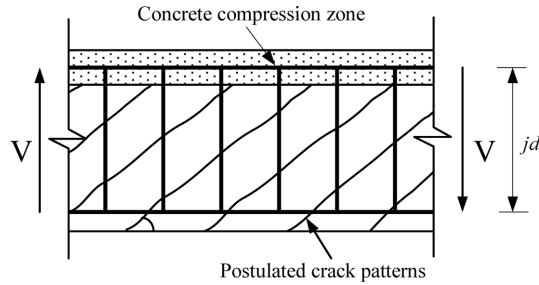


Fig. 2 Shear transfer mechanism for a typical region along a beam member

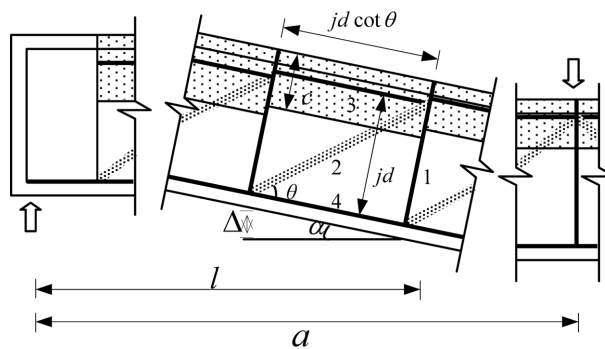


Fig. 3 Typical truss unit analyzed by the principle of virtual work

this analogy, truss units can be formed along the shear span of a cracked slender beam member. In each truss unit, the inclined diagonal strut transfers the shear force to the vertical tension tie. The top and bottom chords are responsible for its flexural resistance. The rigidity and stiffness of each truss unit are then determined by deconstructing the beam shear span. The stiffness of the truss unit is the summation of all the members that form the unit. Using this stiffness, the external work done by each truss unit can be determined. This allows the inclination angle of struts to be examined by minimizing the external work done.

The principle of virtual work is used in the analysis of each truss unit where the axial rigidity of each member forming the truss unit is the most important part and must be studied with care. Consider again the typical truss unit subjected to a shear force  $V$  as shown in Fig. 3, it is assumed that the shear reinforcement is uniformly distributed over the length of the member. Under this smeared shear reinforcement assumption, the axial rigidity of the tension tie is

$$(EA)_t = \cot \theta \rho_w n E_c A_{sa} \tag{1}$$

where  $(EA)_t$  is the axial rigidity of the tension tie;  $\theta$  is the inclination of compression strut;  $\rho_w$  is the shear reinforcement ratio;  $n$  is the modular ratio of  $E_s/E_c$ ;  $E_s$  is the modulus of elasticity for steel;  $E_c$  is the modulus of elasticity for concrete;  $A_{sa}$  is the effective sectional area for shear of RC beam.

For the inclined strut, the cross-sectional area is determined geometrically. Conventionally, it is taken as

$$A_{strut} = b_w j d \cos \theta \quad (2)$$

where  $A_{strut}$  is the cross-sectional area of the inclined strut;  $b_w$  is the beam sectional width;  $jd$  is the flexural lever arm.

Then the axial rigidity of the strut is

$$(EA)_s = b_w j d \cos \theta E_c = \cos \theta E_c A_{sa} \quad (3)$$

where  $(EA)_s$  is the axial rigidity of the strut.

For flexural members, the bottom tensile member is assumed to be at the centroid of the bottom longitudinal bar, while the top compression member is assumed to be at the centroid of the concrete stress block. Hence, the height of the truss is the internal lever arm  $jd$ . A distinction in axial rigidity should also be made between the bottom tensile member and top compressive member. For the tensile member, the concrete in the region is normally cracked and does not contribute significantly to axial rigidity as compared to the regional reinforcement. In addition to concrete stiffness, there is a rigidity contribution from the compression reinforcement located at the top compression member. Usually, the centroid of the compression reinforcement differs from that of the concrete stress block. For simplicity, in this paper, the compression reinforcement is assumed to be at the centroid of the concrete stress block. This simplification may cause a slightly different external work done of the compression reinforcement when the centroid of the stress block for concrete is deeper or shallower than that of the position of the longitudinal reinforcement. Thus, the axial rigidity of the bottom tensile member is

$$(EA)_T = E_s A_s = \rho_s n E_c A_g \quad (4)$$

where  $(EA)_T$  is the rigidity of the bottom tensile member;  $A_s$  is the area of bottom longitudinal reinforcement;  $\rho_s$  is the bottom longitudinal reinforcement ratio,  $\rho_s = A_s / (b_w h)$ ;  $A_g$  is the gross sectional area of reinforced concrete beam.

For the top compression member, the axial rigidity is taken as

$$(EA)_C = (cb_w - A'_s)E_c + A'_s E_s = cb_w E_c + (n-1)A'_s E_s = \left( \frac{c}{h} + \rho'_s (n-1) \right) E_c A_g \quad (5)$$

where  $(EA)_C$  is the axial rigidity of the top compression member;  $c$  is the depth of concrete stress block at the ultimate moment capacity of the beam section;  $h$  is the beam sectional depth;  $A'_s$  is area of top longitudinal reinforcement;  $\rho'_s$  is the top longitudinal reinforcement ratio,  $\rho'_s = A'_s / (b_w h)$ .

These two equations describe the dimensioning of the top and bottom chord members of the truss. Member forces of the truss are found by applying conditions of static equilibrium. As shown in Table 1, principle of virtual work is then applied to determine the deformation of the truss unit.

The deformation of the truss unit is the sum of the member deformations, thus

$$\Delta = \sum_1^4 \frac{Ffl}{EA} = \frac{1 + \frac{\rho_w n}{\sin^4 \theta}}{\rho_w n \cot \theta E_c A_{sa}} j d V + \left( \frac{\left( \frac{l}{jd} - \cot \theta \right)^2 \cot \theta}{\left( \frac{c}{h} + \rho'_s (n-1) \right) E_c A_g} j d V + \frac{\left( \frac{l}{jd} \right)^2 \cot \theta}{\rho_s n E_c A_g} j d V \right) \quad (6)$$

where  $l$  is the updated shear span length;  $V$  is the applied shear force.

Eq. (6) is configured in such a way that the first term is the deformation contribution from shear members (struts and ties) and the second term is that from flexural members. The drift angle is

Table 1 Analysis by the principle of virtual work

| Member | Member force<br>$F$                       | Unit load<br>$f$            | Length<br>$L$           | Axial rigidity<br>( $EA$ )                       |
|--------|---|-----------------------------|-------------------------|--|
| 1      | $V$                                       | 1                           | $jd$                    | $\cot\theta\rho_w n E_c A_{sa}$                  |
| 2      | $-\frac{V}{\sin\theta}$                   | $-\frac{1}{\sin\theta}$     | $\frac{jd}{\sin\theta}$ | $\cos\theta E_c A_{sa}$                          |
| 3      | $\left(\frac{l}{jd} - \cot\theta\right)V$ | $\frac{l}{jd} - \cot\theta$ | $jd\cot\theta$          | $\left(\frac{c}{h} + \rho_s'(n-1)\right)E_c A_g$ |
| 4      | $\frac{l}{jd}V$                           | $\frac{l}{jd}$              | $jd\cot\theta$          | $\rho_s n E_c A_g$                               |

determined by dividing the deformation by the length of the truss unit, thus

$$\alpha = \frac{\Delta}{jd\cot\theta} = \frac{1 + \frac{\rho_w n}{\sin^4\theta}}{\rho_w n \cot^2\theta E_c A_{sa}} V + \left( \frac{\left(\frac{l}{jd} - \cot\theta\right)^2}{\left(\frac{c}{h} + \rho_s'(n-1)\right)E_c A_g} V + \frac{\left(\frac{l}{jd}\right)^2}{\rho_s n E_c A_g} V \right) \quad (7)$$

Therefore, the stiffness of one typical truss unit about the drift angle is

$$K = \frac{V}{\alpha} = \frac{1}{\frac{1 + \frac{\rho_w n}{\sin^4\theta}}{\rho_w n \cot^2\theta E_c A_{sa}} + \frac{\left(\frac{l}{jd} - \cot\theta\right)^2}{\left(\frac{c}{h} + \rho_s'(n-1)\right)E_c A_g} + \frac{\left(\frac{l}{jd}\right)^2}{\rho_s n E_c A_g}} \quad (8)$$

The first term of Eq. (8) represents the shear stiffness of a typical truss unit while the second term represents its flexural stiffness. The first term of Eq. (8) is the same as the shear stiffness presented by Dilger *et al.* (1966) for 90° shear reinforcement of a general truss model. By deriving this shear stiffness term on a typical truss unit in the way shown in Eq. (8), it may not only be taken as shear stiffness for a constant angle truss model, but may also be used as a general description of shear stiffness. Together with the flexural stiffness derived in the expression, a variable angle truss model can be developed.

As noted previously, the inclination of the compression strut  $\theta$  is very important as it affects the shear capacity as well as the stiffness (Eq. (7)) of a RC beam. A theoretical determination of the angle  $\theta$  is needed. From the above analysis, the external work due to an applied unit shear force on the typical truss unit is the total deformation obtained. Thus

$$EWD = \Delta \times 1 = \frac{1 + \frac{\rho_w n}{\sin^4\theta}}{\rho_w n \cot\theta E_c A_{sa}} jd + \left( \frac{\left(\frac{l}{jd} - \cot\theta\right)^2 \cot\theta}{\left(\frac{c}{h} + \rho_s'(n-1)\right)E_c A_g} jd + \frac{\left(\frac{l}{jd}\right)^2 \cot\theta}{\rho_s n E_c A_g} jd \right) \quad (9)$$

The diagonal compression is assumed to develop in the orientation that requires a minimum amount of external energy. Hence, the angle  $\theta$  that minimizes Eq. (9) is the inclination of strut. By differentiating Eq. (9) with respect to  $\theta$  and minimizing the external work done the inclination of strut is found

$$\frac{d(EWD)}{d\theta} = 0 \quad (10)$$

Carrying out the differentiation of Eq. (10) leads to the following solution for the crack angle  $\theta$

$$\begin{aligned} & \left( \frac{1}{\rho_w n E_c A_{sa}} + \frac{1}{E_c A_{sa}} \right) \tan^4 \theta - \left( \frac{2}{E_c A_{sa}} + \frac{\left(\frac{l}{jd}\right)^2}{\left(\frac{c}{h} + \rho_s' (n-1)\right) E_c A_g} + \frac{\left(\frac{l}{jd}\right)^2}{\rho_s n E_c A_g} \right) \tan^2 \theta \\ & + \frac{4\left(\frac{l}{jd}\right)}{\left(\frac{c}{h} + \rho_s' (n-1)\right) E_c A_g} \tan \theta - \left( \frac{3}{\left(\frac{c}{h} + \rho_s' (n-1)\right) E_c A_g} + \frac{3}{E_c A_{sa}} \right) = 0 \end{aligned} \quad (11)$$

Eq. (11) is a four degree-one variable equation in  $\theta$ . An analytical solution of this equation is possible; however, a trial and error procedure is sufficient.

The solutions of  $\theta$  vary along the shear span of the beam as the variable  $l$ , which represents the available shear span length, is different for each truss unit. For a particular shear level, the solution procedure starts from the loading point and moves towards the support in a shear span. According to Eq. (11),  $\theta$  for the first truss unit can be found by substituting the total shear span length  $a$  to the variable  $l$ . With this  $\theta$  value, a check of  $jd \cot \theta$  which represents the length of this unit truss can be done. If the result shows that  $jd \cot \theta$  is smaller than  $a$ , the solution procedure should continue for the next truss unit by updating the variable  $l$  with a new value ( $a - jd \cot \theta$ ). Then  $\theta$  for the next truss unit can be obtained with Eq. (11) again. The process will be terminated when the check shows that the variable  $l$  used to calculate  $\theta$  for a new truss unit is smaller than the length ( $jd \cot \theta$ ) of this newly formed truss unit (i.e., available shear span length is not enough for a new truss unit). So the solutions of the inclination of struts for truss units along the shear span of the beam differ in a decreasing manner when moving towards the support as the variable  $l$  gets smaller. Moreover, when the shear increases, a few variables such as  $c$  in Eq. (11) are also affected, and hence the solutions of the inclination of struts are different. Thus, a continuous profile of struts orientation development can be found in this analysis. Fig. 4 shows the results of this analysis at the ultimate stage of a RC beam. The beam and the crack pattern were extracted from Bresler and Scordelis (1963).

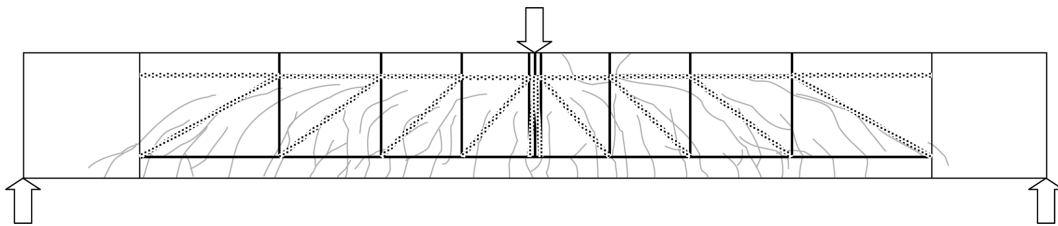


Fig. 4 Comparison of calculated  $\theta$  and observed angle of cracks for Beam A-2 (Bresler *et al.* 1963)

In summary, this theoretical method has two distinct characteristics for the evaluation of  $\theta$ . Firstly, inclinations of the struts calculated from this method are different along the shear span from the load point to the support (i.e., different inclination of strut for different truss unit). This effectively produces a variable angle truss model for the reinforced concrete beam. Secondly, inclination of the struts can vary with increasing shear force level. Thus, the change of direction in the development of diagonal compression can be seen. This intends to correspond with the crack patterns observed in most of the RC beam tests.

### 3. Strain compatibility

Shear carried by concrete has long been recognized as an important portion of the shear strength of a reinforced concrete member. Some research has tried to use other parameters to represent this concrete contribution. But amongst all these parameters, transverse tensile stress and strain have prevailed (Vecchio *et al.* 1986). In this paper, the concrete contribution is assumed as the amount of force transferred across cracks, as shown in Fig. 5. Transverse tensile stress and strain were used to indirectly incorporate this amount of force transferred across cracks into the shear strength of reinforced concrete beams through the compatibility conditions. By assuming a uniform distribution of transverse reinforcement along cracks and that the tensile strain in the transverse direction is equal to the strain in the transverse reinforcement, the tensile strain in the transverse direction can be calculated as

$$\epsilon_y = \frac{V_s s}{A_v E_s j d \cot \theta} \tag{12}$$

where  $\epsilon_y$  is the strain in  $y$ -direction;  $V_s$  is the shear strength contribution from shear reinforcement;  $s$  is the spacing of transverse reinforcements.

The principal stress directions are the direction of inclined strut ( $\theta$ ). At this stage, the element has a compressive stress along the strut direction and a tensile stress perpendicular to it. However, the directions of the principal strains deviate from the principal stress directions. Vecchio and Collins (1986) have summarized a number of experimental data and found that the direction of the principal strains only differed from the principal stresses by  $\pm 10^\circ$ . Therefore, it is reasonable to assume that the principal stress and strain directions for an infinitesimal element of concrete coincide with each other. The principal strain in the compressive direction is readily determined by the stress and geometrical condition of a strut as illustrated in Fig. 5, thus

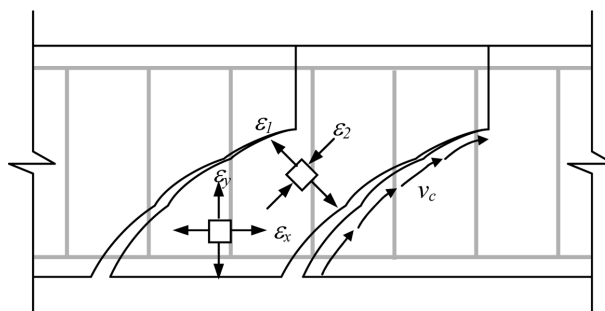


Fig. 5 Local stresses and strains at a crack

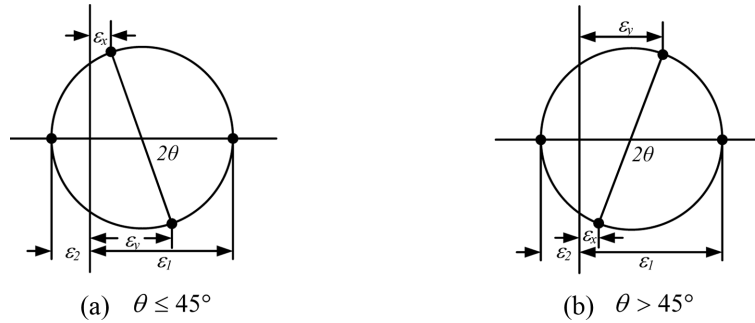


Fig. 6 Compatible strain conditions in a RC element

$$\varepsilon_2 = -\frac{V}{jdb_w E_c \sin \theta \cos \theta} = -\frac{V_s + V_c}{jdb_w E_c \sin \theta \cos \theta} \quad (13)$$

where  $\varepsilon_2$  is the principle compressive strain in concrete.

With the known values of  $\theta$ ,  $\varepsilon_y$ , and  $\varepsilon_2$ , a Mohr's circle can then be constructed as shown in Fig. 6 to calculate the tensile strain  $\varepsilon_1$ , given below

$$\varepsilon_1 = \frac{2(\varepsilon_y + \varepsilon_2)}{|\cos 2\theta| + 1} - \varepsilon_2 \quad (14)$$

This equation takes into consideration that  $\theta$  may be more than  $45^\circ$ .

Many researchers including Walraven *et al.* (1981) have concentrated on the experimental relationships between the shear carried by concrete  $v_c$  and the tensile strain  $\varepsilon_1$ . Vecchio and Collins (1986) derived the equation for the limiting value of shear stress transferred across the crack; the equation further used by Walraven *et al.* (1981) in his study is given below

$$v_c = \frac{0.18\sqrt{f'_c}}{0.31 + 24\frac{w}{a^* + 16}} + 1.64f_{ci} - 0.82\frac{f_{ci}^2}{\frac{\sqrt{f'_c}}{0.31 + 24\frac{w}{a^* + 16}}} \quad (15)$$

where  $a^*$  is the maximum aggregate size in millimeters;  $f_{ci}$  is the compressive stress on crack surface (assumed as zero in this model);  $f'_c$  is the compressive strength of concrete and  $w$  is the average crack width over the cracked surface. The crack width can be taken as

$$w = \varepsilon_1 s_\theta \quad (16)$$

Where

$$s_\theta = \frac{1}{\frac{\sin \theta}{s_{mx}} + \frac{\cos \theta}{s_{my}}} \quad (17)$$

and where  $s_{mx}$  and  $s_{my}$  are the indicators of the crack control characteristics of the longitudinal and transverse shear reinforcement, respectively. Bhide and Collins (1989) used the provision of the CEB-FIP Code (1978) for calculating the crack spacing

$$s_{mx} = 2\left(c_x + \frac{s_x}{10}\right) + 0.25k_1 \frac{d_{bx}}{\rho_s} \quad (18)$$

$$s_{my} = 2\left(c_y + \frac{s}{10}\right) + 0.25k_1 \frac{d_{by}}{\rho_w} \quad (19)$$

where  $k_1$  is equal to 0.4 for deformed reinforcing bars or 0.8 for plain reinforcing bars;  $c_x$  is the distance to longitudinal reinforcement;  $c_y$  is the distance to shear reinforcement;  $d_{bx}$  is the bar diameter of longitudinal reinforcement;  $d_{by}$  is the bar diameter of shear reinforcement.

The calculated  $v_c$  from Eq. (15) is the shear stress transferred at cracks surface. In the truss model proposed in this paper, crack surface can be approximated along the strut direction. Hence the shear strength contributed from concrete is

$$V_c = \frac{jdb_w}{\sin\theta} v_c \sin\theta = jdb_w v_c \quad (20)$$

Additional contribution to the truss unit from transverse reinforcement can be defined as

$$V_s = \cot\theta A_v f_y \frac{jd}{s} \quad (21)$$

This paper is based on the premise that the stirrups yield when shear failure occurs in the slender RC beams. As we know, the height of the compressive zone of the section decreases rapidly after the stirrups yielding, and there is a rapidly increasing compressive stress of the diagonal concrete strut, till the strut crushes. Because all the shear failure modes belong to brittle failure, the actual shear strength at shear compression failure is a little higher than the shear force at stirrups yielding. The shear force at stirrups yielding is taken as the shear strength, which is a little conservative for design but without sacrificing accuracy.

#### 4. Solution algorithm for shear strength

In the previous sections of this paper, inclinations of struts and concrete contribution have been addressed for the variable-angle truss model theoretically. The method to develop the variable-angle truss model and treatment of the concrete contribution can be verified by predicting the shear strength of RC beams subjected to shear. The strength of each truss unit of the variable-angle truss model is made up of two portions:  $V_s$  and  $V_c$ .  $V_s$  is the shear reinforcement contribution which will cause a deformation in each truss unit. Consequently, it mobilizes  $V_c$  (the shear carried by concrete) in the truss unit. At a low shear level,  $V_c$  calculated from Eq. (20) may be larger than the applied shear force. This probably explains why the concrete has not been cracked and only part of the  $V_c$  mechanism has been utilized. At this point, shear reinforcement might not participate in the shear resistance. At a higher shear level,  $V_c$  is fully utilized first and then followed by the shear reinforcement subjected to the shear stress generated. With an increase in the load level, the transverse reinforcements may eventually yield. In this model, each truss unit is assumed to reach its shear strength when the transverse reinforcements of that truss unit yield. The yield strain of steel is assumed as  $f_y/E_s$  to calculate  $V_c$  at the failure state. The compression softening of the concrete and tension stiffening of the reinforcement were ignored implying that original properties

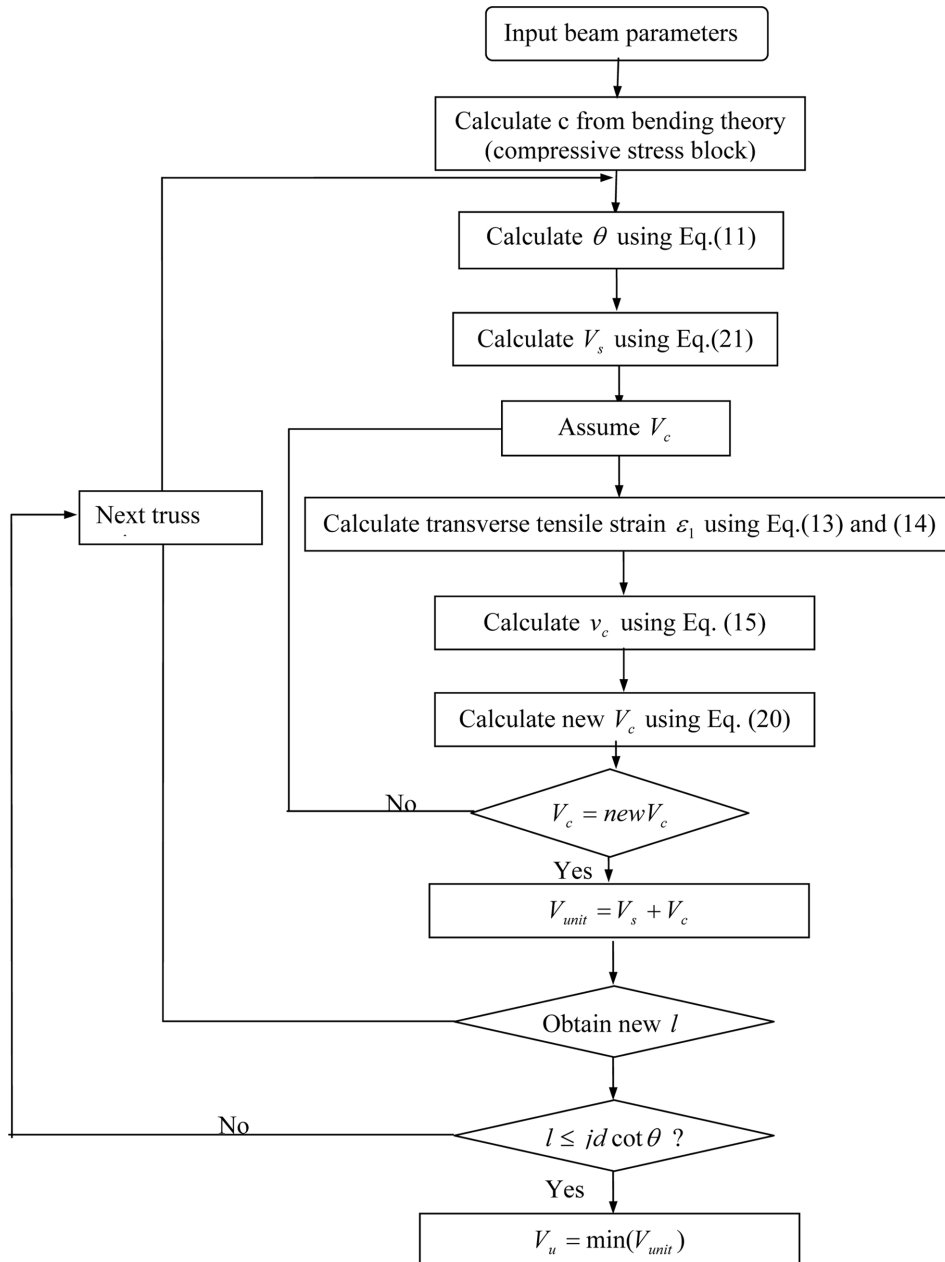


Fig. 7 Flowchart showing the solution algorithm for shear strength

of steel and concrete were used in the model. The shear strength of RC beams is defined as the minimum value of the shear strength of every truss unit of RC beams. The step-by-step solution process is summarized in the flowchart shown in Fig. 7. The MatLab (Rudra *et al.* 2006) program was used to solve the flowchart.

Table 2 Experimental verification

|  | Beam No.  | $f'_c$<br>(MPa) | $b$<br>(mm) | $h$<br>(mm) | $a$<br>(mm) | $\frac{a}{d}$ | $\rho'_s$<br>(%) | $\rho_s$<br>(%) | $\rho_w$<br>(%) | $\left(\frac{\theta_{exp}}{\theta_{Model}}\right)$ | $\left(\frac{\theta_{exp}}{\theta_{AASHTO}}\right)$ | $\left(\frac{\theta_{exp}}{\theta_{CSA}}\right)$ | $V_{exp}$<br>(kN) | $V_{Model}$<br>(kN) | $\frac{V_{exp}}{V_{Model}}$ | $\frac{V_{exp}}{V_{MCFT}}$ |
|--|-----------|-----------------|-------------|-------------|-------------|---------------|------------------|-----------------|-----------------|--|---|--|-------------------|---------------------|-----------------------------|----------------------------|
| Bresler <i>et al.</i><br>(1963)          | A2        | 24.3            | 305         | 559         | 2285        | 4.4           | 0.15             | 1.89            | 0.10            | 1.05   | 1.39  | 1.36   | 244.5             | 181.1               | 1.35                        | 1.32                       |
|  | A3        | 35.1            | 307         | 561         | 3200        | 6.2           | 0.15             | 2.25            | 0.10            | 0.9  | 1.4   | 1.32   | 233.5             | 212.3               | 1.10                        | 1.16                       |
| Vecchio <i>et al.</i><br>(2004)          | A1        | 22.6            | 305         | 552         | 1830        | 3.7           | 0.18             | 1.43            | 0.10            | 0.85   | 1.06  | 1.02   | 229.5             | 156.1               | 1.47                        | 0.97                       |
|  | A2        | 25.9            | 305         | 552         | 2285        | 4.6           | 0.18             | 1.78            | 0.10            | 1.1  | 1.5   | 1.36   | 219.5             | 166.3               | 1.32                        | 0.99                       |
|  | A3        | 43.5            | 305         | 552         | 3200        | 6.5           | 0.18             | 2.14            | 0.04            | 1.18   | 1.44  | 1.26   | 210.0             | 178.0               | 1.18                        | 1.18                       |
|  | B1        | 22.6            | 229         | 552         | 1830        | 3.7           | 0.24             | 1.90            | 0.15            | 0.87   | 1.17  | 1.01   | 217.0             | 142.8               | 1.52                        | 1.04                       |
|  | B2        | 25.9            | 229         | 552         | 2285        | 4.6           | 0.24             | 1.90            | 0.15            | 0.9  | 1.35  | 1.14   | 182.5             | 149.6               | 1.22                        | 1.06                       |
|  | B3        | 43.5            | 229         | 552         | 3200        | 6.5           | 0.24             | 2.38            | 0.06            | 1.09   | 1.46  | 1.32   | 171.0             | 148.7               | 1.15                        | 1.11                       |
|  | C1        | 22.6            | 152         | 552         | 1830        | 3.7           | 0.36             | 1.67            | 0.20            | 0.99   | 1.5   | 1.2  | 141.0             | 108.5               | 1.30                        | 1.10                       |
|  | C2        | 25.9            | 152         | 552         | 2285        | 4.6           | 0.36             | 2.86            | 0.20            | 0.71   | 1.06  | 0.92   | 145.0             | 122.9               | 1.18                        | 1.22                       |
| Al-Nahlawi <i>et al.</i><br>(1989, 1992) | S.6.8-110 | 46.5            | 152         | 406         | 711         | 2.0           | 0.06             | 1.23            | 0.14            | 1.28   | 1.58  | 1.02   | 149.1             | 95.6                | 1.56                        | 1.33                       |
|  | S-8-110   | 55.1            | 152         | 406         | 711         | 2.0           | 0.06             | 1.23            | 0.14            | 1.06   | 1.24  | 0.83   | 193.5             | 102.4               | 1.89                        | 1.61                       |
|  | S-11-110  | 73.0            | 152         | 406         | 711         | 2.0           | 0.06             | 1.23            | 0.14            | 0.95   | 0.98  | 0.74   | 144.6             | 115.7               | 1.25                        | 1.14                       |
| Placas <i>et al.</i><br>(2003)           | R8        | 26.7            | 152         | 305         | 914         | 3.4           | 0.34             | 1.46            | 0.21            | 1.03   | 1.53  | 1.19   | 79.6              | 73.0                | 1.09                        | 1.05                       |
|  | R9        | 29.6            | 152         | 305         | 914         | 3.4           | 0.34             | 1.46            | 0.43            | 1.08   | 1.9   | 1.44   | 104.5             | 90.9                | 1.15                        | 1.27                       |
|  | R16       | 31.6            | 152         | 305         | 979         | 3.6           | 2.95             | 4.15            | 0.43            | 0.93   | 1.35  | 1.37   | 139.7             | 99.1                | 1.41                        | 1.19                       |
|  | R28       | 31.6            | 152         | 305         | 979         | 3.6           | 2.95             | 4.15            | 0.83            | 0.87   | 1.48  | 1.25   | 179.3             | 122                 | 1.47                        | 1.19                       |
| Tompos <i>et al.</i><br>(2002)           | V36-2     | 27.5            | 457         | 915         | 2553        | 3.0           | 0.03             | 0.92            | 0.08            | 1.15   | 1.32  | 1.08   | 487.5             | 369.3               | 1.32                        | 1.14                       |
|  | V36-3     | 27.5            | 457         | 915         | 2553        | 3.0           | 0.03             | 0.92            | 0.08            | 0.97   | 1.13  | 0.89   | 511.5             | 368.0               | 1.39                        | 1.19                       |
|  | V18-2     | 27.5            | 229         | 486         | 1276        | 3.0           | 0.13             | 0.91            | 0.15            | 1.11   | 1.54  | 1.25   | 172.1             | 123.8               | 1.39                        | 1.01                       |
|  | V18-2c    | 27.5            | 229         | 486         | 1276        | 3.0           | 0.13             | 0.91            | 0.15            | 1.06   | 1.47  | 1.22   | 153.0             | 124.4               | 1.23                        | 0.89                       |
|  | V18-3     | 27.5            | 229         | 486         | 1276        | 3.0           | 0.13             | 0.91            | 0.33            | 0.99   | 1.71  | 1.18   | 276.7             | 158.1               | 1.75                        | 1.59                       |
| Karayiannis <i>et al.</i><br>(1999)      | B90       | 26.0            | 200         | 300         | 900         | 3.5           | 0.59             | 1.97            | 0.13            | 1.12   | 1.31  | 1.28   | 84.8              | 71.3                | 1.19                        | 1.22                       |
| Cladera <i>et al.</i> (2005)             | H60/3     | 60.8            | 200         | 400         | 1080        | 3.1           | 0.13             | 2.01            | 0.24            | 1.04   | 1.36  | 1.17   | 259.0             | 153.3               | 1.69                        | 1.15                       |

Table 2 Continued

|                                   | Beam No. | $f'_c$<br>(MPa) | $b$<br>(mm) | $h$<br>(mm) | $a$<br>(mm) | $\frac{a}{d}$ | $\rho'_s$<br>(%) | $\rho_s$<br>(%) | $\rho_w$<br>(%) | $\left(\frac{\theta_{exp}}{\theta_{Model}}\right)$ | $\left(\frac{\theta_{exp}}{\theta_{AASHTO}}\right)$ | $\left(\frac{\theta_{exp}}{\theta_{CSA}}\right)$ | $V_{exp}$<br>(kN) | $V_{Model}$<br>(kN) | $\frac{V_{exp}}{V_{Model}}$ | $\frac{V_{exp}}{V_{MCFT}}$ |
|-----------------------------------|----------|-----------------|-------------|-------------|-------------|---------------|------------------|-----------------|-----------------|--|---|--|-------------------|---------------------|-----------------------------|----------------------------|
| Kong <i>et al.</i><br>(1998)      | S2-1     | 72.5            | 250         | 350         | 730         | 2.5           | 0.26             | 2.34            | 0.11            | 0.98   | 0.78  | 0.8  | 260.3             | 159.5               | 1.63                        | 1.53                       |
|                                   | S2-2     | 72.5            | 250         | 350         | 730         | 2.5           | 0.26             | 2.34            | 0.13            | 1.02   | 0.85  | 0.86   | 232.5             | 166.3               | 1.40                        | 1.19                       |
|                                   | S2-3     | 72.5            | 250         | 350         | 730         | 2.5           | 0.26             | 2.34            | 0.16            | 1.08   | 0.98  | 0.97   | 253.3             | 171.1               | 1.48                        | 1.16                       |
|                                   | S2-4     | 72.5            | 250         | 350         | 730         | 2.5           | 0.26             | 2.34            | 0.16            | 1.08   | 0.98  | 0.93   | 219.4             | 171.1               | 1.28                        | 1.01                       |
|                                   | S2-5     | 72.5            | 250         | 350         | 730         | 2.5           | 0.26             | 2.34            | 0.21            | 0.88   | 0.88  | 0.81   | 282.1             | 180.1               | 1.57                        | 1.12                       |
|                                   | S3-1     | 67.4            | 250         | 350         | 730         | 2.5           | 0.26             | 1.41            | 0.10            | 0.97   | 0.88  | 0.83   | 209.2             | 133.9               | 1.56                        | 1.21                       |
|                                   | S3-2     | 67.4            | 250         | 350         | 730         | 2.5           | 0.26             | 1.41            | 0.10            | 0.97   | 0.88  | 0.83   | 178.1             | 133.9               | 1.33                        | 1.03                       |
|                                   | S3-3     | 67.4            | 250         | 350         | 730         | 2.5           | 0.26             | 2.34            | 0.10            | 0.88   | 0.68  | 0.69   | 228.6             | 159.1               | 1.44                        | 1.30                       |
|                                   | S3-4     | 67.4            | 250         | 350         | 730         | 2.5           | 0.26             | 2.34            | 0.10            | 0.88   | 0.68  | 0.69   | 174.9             | 159.1               | 1.10                        | 1.01                       |
|                                   | S3-5     | 67.4            | 250         | 350         | 720         | 2.4           | 0.26             | 3.15            | 0.10            | 1.10   | 0.83  | 0.83   | 296.6             | 164.7               | 1.80                        | 1.62                       |
|                                   | S3-6     | 67.4            | 250         | 350         | 720         | 2.4           | 0.26             | 3.15            | 0.10            | 1.10   | 0.83  | 0.83   | 282.9             | 164.7               | 1.72                        | 1.54                       |
|                                   | S5-1     | 89.4            | 250         | 350         | 880         | 3.0           | 0.26             | 2.34            | 0.16            | 1.05   | 1.09  | 1.05   | 241.7             | 174.6               | 1.38                        | 1.12                       |
|                                   | S5-2     | 89.4            | 250         | 350         | 800         | 2.7           | 0.26             | 2.34            | 0.16            | 1.1  | 1.06  | 1.06   | 259.9             | 181.1               | 1.44                        | 1.20                       |
| S5-3                              | 89.4     | 250             | 350         | 730         | 2.5         | 0.26          | 2.34             | 0.16            | 0.78            | 0.71   | 0.7   | 243.8  | 186.5             | 1.31                | 1.13                        |                            |
| Ozcebe <i>et al.</i><br>(1999)    | S-59-ACI | 82.0            | 150         | 360         | 1625        | 5.0           | 0.29             | 3.81            | 0.14            | 0.63   | 0.82  | 0.77   | 96.5              | 139.9               | 0.69                        | 1.05                       |
|                                   | S-59-TH  | 75.0            | 150         | 360         | 1625        | 5.0           | 0.29             | 3.81            | 0.19            | 0.95   | 1.35  | 1.34   | 119.3             | 143.7               | 0.83                        | 1.12                       |
|                                   | S-59-TS  | 82.0            | 150         | 360         | 1625        | 5.0           | 0.29             | 3.81            | 0.28            | 0.84   | 1.32  | 1.18   | 125.4             | 169.5               | 0.74                        | 0.93                       |
|                                   | S-39-ACI | 73.0            | 150         | 360         | 975         | 3.0           | 0.29             | 3.81            | 0.14            | 1.06   | 0.97  | 0.91   | 111.8             | 141.5               | 0.79                        | 1.20                       |
|                                   | S-39-TH  | 73.0            | 150         | 360         | 975         | 3.0           | 0.29             | 3.81            | 0.21            | 1.1  | 1.24  | 1.12   | 142.9             | 148.9               | 0.96                        | 1.20                       |
|                                   | S-39-TS  | 73.0            | 150         | 360         | 975         | 3.0           | 0.29             | 3.81            | 0.28            | 0.94   | 1.05  | 1.09   | 179.2             | 162.9               | 1.10                        | 1.25                       |
| Narayanan <i>et al.</i><br>(1988) | SS4      | 43.3            | 85          | 150         | 262         | 2.0           | 0.91             | 1.99            | 0.21            | 0.99   | 0.93  | 0.98   | 32.0              | 29.1                | 1.10                        | 1.08                       |
| Johnson <i>et al.</i><br>(1989)   | Beam 7   | 51.3            | 305         | 610         | 1670        | 3.1           | 0.69             | 2.20            | 0.07            | 1.43   | 1.14  | 1.2  | 317.7             | 269.2               | 1.18                        | 1.11                       |
|                                   | Beam 5   | 55.8            | 305         | 610         | 1670        | 3.1           | 0.69             | 2.20            | 0.14            | 1.23   | 1.3   | 1.29   | 433.0             | 311.5               | 1.39                        | 0.95                       |

Table 2 Continued

|                               | Beam No. | $f'_c$<br>(MPa) | $b$<br>(mm) | $h$<br>(mm) | $a$<br>(mm) | $\frac{a}{d}$ | $\rho'_s$<br>(%) | $\rho_s$<br>(%) | $\rho_w$<br>(%) | $\left(\frac{\theta_{exp}}{\theta_{Model}}\right)$ | $\left(\frac{\theta_{exp}}{\theta_{AASHTO}}\right)$ | $\left(\frac{\theta_{exp}}{\theta_{CSA}}\right)$ | $V_{exp}$<br>(kN) | $V_{Model}$<br>(kN) | $\frac{V_{exp}}{V_{Model}}$ | $\frac{V_{exp}}{V_{MCFT}}$ |
|-------------------------------|----------|-----------------|-------------|-------------|-------------|---------------|------------------|-----------------|-----------------|--|---|--|-------------------|---------------------|-----------------------------|----------------------------|
| Rahal <i>et al.</i><br>(2004) | A65-200  | 60.9            | 200         | 370         | 900         | 2.8           | 0.31             | 1.99            | 0.14            | 0.83   | 0.68  | 0.85   | 175.0             | 131.6               | 1.33                        | 1.45                       |
|                               | A65-140  | 62.1            | 200         | 370         | 900         | 2.8           | 0.31             | 1.99            | 0.20            | 1.11   | 1.28  | 1.22   | 150.0             | 150.0               | 1.00                        | 1.11                       |
|                               | A65-110  | 60.9            | 200         | 370         | 900         | 2.8           | 0.31             | 1.99            | 0.26            | 0.55   | 0.69  | 0.69   | 188.0             | 164.9               | 1.14                        | 1.16                       |
|                               | A65-95   | 62.1            | 200         | 370         | 900         | 2.8           | 0.31             | 1.99            | 0.30            | 0.93   | 1.22  | 1.17   | 220.0             | 176.0               | 1.25                        | 1.27                       |
|                               | B65-160  | 65.1            | 200         | 370         | 900         | 3.0           | 0.31             | 3.32            | 0.18            | 0.83   | 0.88  | 0.83   | 208.0             | 135.1               | 1.54                        | 1.54                       |
|                               | B65-140  | 65.1            | 200         | 370         | 900         | 3.0           | 0.31             | 3.32            | 0.20            | 0.96   | 1.02  | 1  | 235.0             | 136.6               | 1.72                        | 1.61                       |
|                               | B65-125  | 66.4            | 200         | 370         | 900         | 3.0           | 0.31             | 3.32            | 0.23            | 1.27   | 1.4   | 1.36   | 242.0             | 143.2               | 1.69                        | 1.54                       |
|                               | B65-110  | 66.4            | 200         | 370         | 900         | 3.0           | 0.31             | 3.32            | 0.26            | 0.92   | 1.02  | 1.01   | 270.0             | 150.8               | 1.79                        | 1.69                       |
| Rahal <i>et al.</i><br>(2006) | S1-25-05 | 24.3            | 210         | 400         | 1020        | 3.0           | 0.37             | 2.34            | 0.28            | 1.11   | 1.47  | 1.34   | 166.0             | 127.7               | 1.30                        | 0.92                       |
|                               | S2-25-25 | 25.3            | 250         | 400         | 1020        | 3.0           | 0.31             | 1.96            | 0.24            | 1.01   | 1.3   | 1.21   | 194.0             | 141.6               | 1.37                        | 0.94                       |
|                               | S3-25-50 | 27.3            | 300         | 400         | 1020        | 3.0           | 0.26             | 1.64            | 0.19            | 0.85   | 1.07  | 0.93   | 199.0             | 156.7               | 1.27                        | 0.84                       |
|                               | S4-25-75 | 25.3            | 350         | 400         | 1020        | 3.0           | 0.22             | 1.40            | 0.17            | 0.92   | 1.17  | 1.08   | 244.0             | 160.5               | 1.52                        | 0.99                       |
|                               | S2-40-25 | 43.1            | 250         | 400         | 1020        | 3.0           | 0.31             | 1.96            | 0.24            | 1.06   | 1.36  | 1.24   | 257.0             | 169.1               | 1.52                        | 1.02                       |
|                               | S3-40-50 | 41.6            | 300         | 400         | 1020        | 3.0           | 0.26             | 1.64            | 0.19            | 1.08   | 1.35  | 1.35   | 262.0             | 178.2               | 1.47                        | 1.04                       |
|                               | S4-40-75 | 42.2            | 350         | 400         | 1020        | 3.0           | 0.22             | 1.40            | 0.17            | 1.05   | 1.33  | 1.29   | 264.0             | 187.2               | 1.41                        | 1.02                       |
| Yoon <i>et al.</i><br>(1996)  | N1N      | 36.0            | 375         | 750         | 2150        | 3.2           | 0.06             | 2.51            | 0.08            | 1.14   | 0.98  | 0.99   | 457.0             | 357.0               | 1.28                        | 1.35                       |
|                               | M1N      | 67.0            | 375         | 750         | 2150        | 3.1           | 0.06             | 2.51            | 0.08            | 1.19   | 0.98  | 1.03   | 405.0             | 470.9               | 0.86                        | 1.10                       |
|                               | H1N      | 87.0            | 375         | 750         | 2150        | 3.1           | 0.06             | 2.51            | 0.08            | 1.18   | 0.97  | 0.98   | 483.0             | 519.4               | 0.93                        | 1.35                       |
|                               | N2S      | 36.0            | 375         | 750         | 2150        | 3.1           | 0.06             | 2.51            | 0.08            | 1.18   | 1.05  | 1.02   | 363.0             | 349.0               | 1.04                        | 1.11                       |
|                               | N2N      | 36.0            | 375         | 750         | 2150        | 3.1           | 0.06             | 2.51            | 0.12            | 0.96   | 0.92  | 0.97   | 483.0             | 365.9               | 1.32                        | 1.27                       |
|                               | M2S      | 67.0            | 375         | 750         | 2150        | 3.1           | 0.06             | 2.51            | 0.12            | 0.81   | 0.78  | 0.77   | 552.0             | 480.0               | 1.15                        | 1.49                       |
|                               | M2N      | 67.0            | 375         | 750         | 2150        | 3.1           | 0.06             | 2.51            | 0.16            | 1.2  | 1.29  | 1.14   | 689.0             | 510.4               | 1.35                        | 1.18                       |
|                               | H2S      | 87.0            | 375         | 750         | 2150        | 3.1           | 0.06             | 2.51            | 0.12            | 1.05   | 1.01  | 0.93   | 598.0             | 533.9               | 1.12                        | 1.32                       |
|                               | H2N      | 87.0            | 375         | 750         | 2150        | 3.1           | 0.06             | 2.51            | 0.23            | 0.97   | 1.18  | 0.99   | 721.0             | 655.5               | 1.10                        | 1.03                       |
| Average                       |          |                 |             |             |             |               |                  |                 |                 | 0.97   | 1.15  | 1.06   |                   |                     | 1.24                        | 1.14                       |
| CoV                           |          |                 |             |             |             |               |                  |                 |                 | 0.15   | 0.27  | 0.2  |                   |                     | 0.24                        | 0.18                       |

Note: CoV= coefficient of variation.

## 5. Comparison with test results

The validation of the proposed truss approach is demonstrated by comparison with published experimental results from previous investigations with respect to the shear strength and inclination angle of compression strut at this state. Details of the RC beams can be found in Table 2. These beams encompass a wide range of sizes and material properties. The beams selected were shear-critical flexural members. The shear strength of RC beams in the proposed model is governed by the strength of the transverse reinforcements plus the shear transferred across the cracks. In order to verify the proposed model, only the lightly shear-reinforced beams with aspect ratios larger than 2 were selected. The reinforced concrete beams with aspect ratios smaller than 2 or thin web, in which the diagonal cracking strength govern the shear strength of the beams, were excluded. Among the shear-critical flexural beams, only those with cracking patterns provided were selected. The model does not apply to beams which are over-reinforced, and to beams with inadequate transverse reinforcement.

### 5.1 Inclination angle of compression strut

Fig. 8 shows the comparison between calculated inclinations of struts and the experimentally recorded crack patterns for sample beams presented in Table 2. In these graphs of Fig. 8, the strut inclinations are observed to have similar orientations as the cracks developed. The analytical results revealed that the proposed variable-truss angle model was capable of capturing crack patterns of RC beams with satisfactory accuracy. To further demonstrate the capacity of the proposed variable-truss angle model in capturing the inclination angle of compression struts along the RC beams, the maximum inclination angle of compression strut observed from the experiments was compared with the analytical result as showed in Fig. 9. Overall, the average value of the experimental to predicted shear-critical angle by the proposed approach is 0.97.

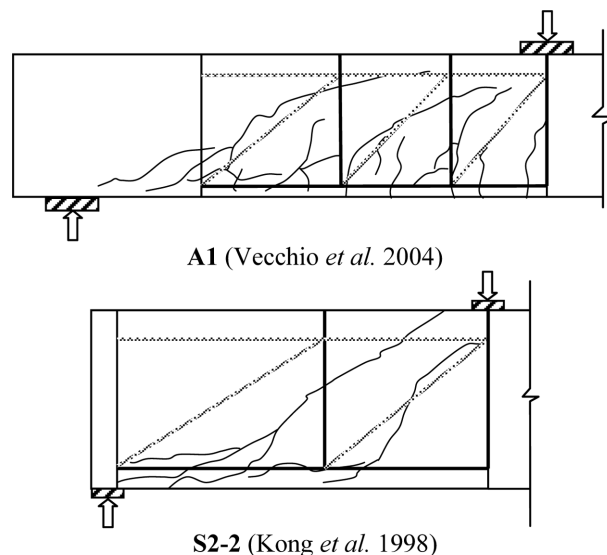


Fig. 8 Comparison of calculated  $\theta$  and observed angle of crack for sample beams

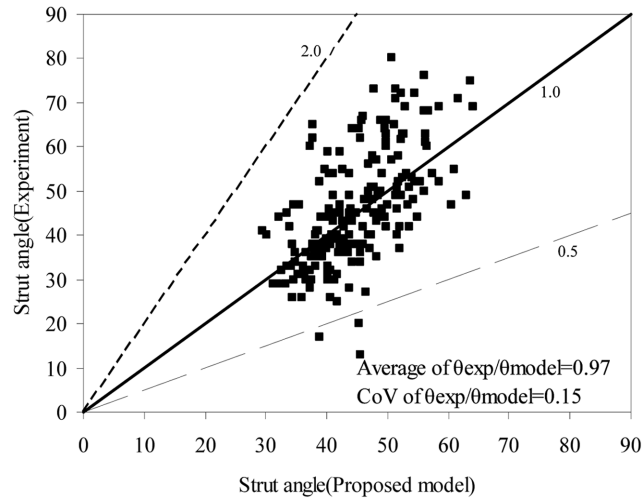


Fig. 9 Correlation of maximum experimental and predicted inclination of compression strut based on the proposed method

The inclined angle of shear-critical beams in the database calculated based on the proposed model, AASHTO (2004), and CSA (2004) are shown in Table 2. The mean ratio of the experimental to predicted angle and its coefficient of variation are 0.97 and 0.15, 1.15 and 0.27, 1.06 and 0.20 for the proposed model, AASHTO (2004), and CSA (2004), respectively. Comparison of available models with experimental data indicates that the proposed model produce better mean ratio of the experimental to predicted strength than the AASHTO (2004), and CSA (2004). The results of the calculated angles by Eq. (11) are shown to be consistent with the experimentally observed angles of the shear-critical RC beams.

### 5.2 Shear strength

The shear strengths from the proposed method and experimental results were compared as shown in Fig. 10. The average value of the experimental to predicted shear strength by the proposed model is 1.24, showing a fairly good correlation between the proposed variable-truss angle model and the experimental data. Importantly, most of the analytical results based on the proposed method were on the safe side as illustrated in Fig. 10. This is due to not taking into account the dowel action and shear carried by the compression zone in the concrete contribution. The proposed model could be used to give a lower bound for the shear capacity of the available experimental data.

Beside the analytical results according to the proposed variable-truss angle model, the predicted shear strengths based on modified compression field theory (MCFT) (Bentz *et al.* 2000) are also presented in Fig. 11. The Response program (Bentz *et al.* 2000) was used to calculate the predicted shear strengths. While it can be seen that MCFT (Bentz *et al.* 2000) shows good accuracy with the average value of the ratio being 1.14, it is of interest to explore the development of a new model that is able to explain the shear behavior of RC beams. It is believed that the method presented in this paper gives a physical significance to the parameters being calculated. The shear strengths of shear-critical beams in the database calculated based on the proposed model, MCFT (Bentz *et al.* 2000),

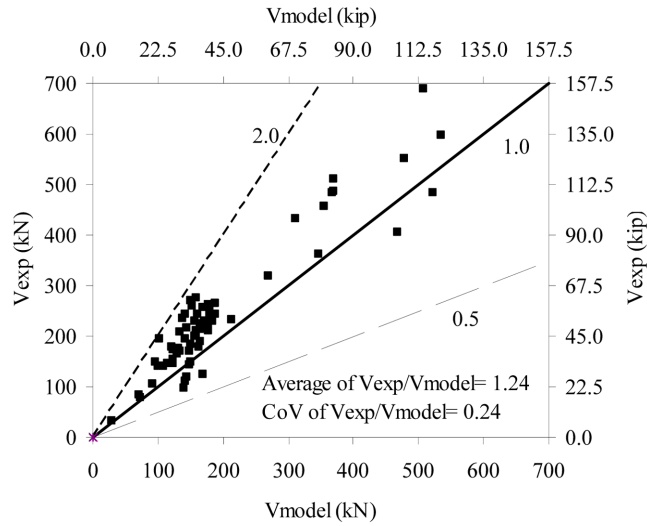


Fig. 10 Correlation of experimental and predicted shear strength based on the proposed method

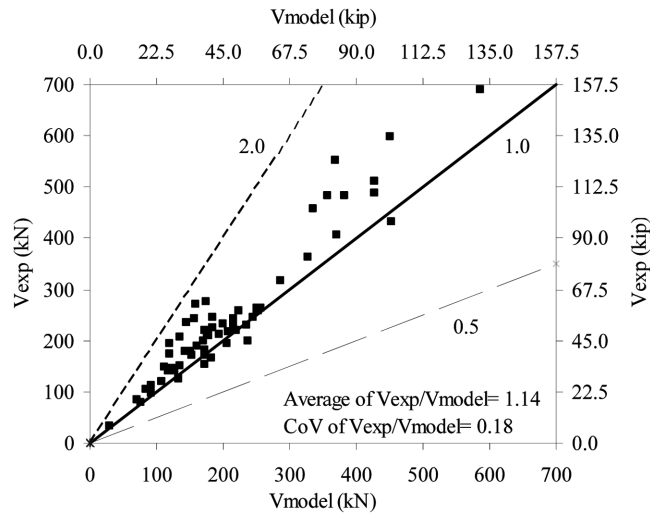


Fig. 11 Correlation of experimental and predicted shear strength based on MCFT (Bentz *et al.* 2000)

Table 3 Verification of different shear procedures for shear-critical RC beams

|         | $\frac{V_{exp}}{V_{Model}}$ | $\frac{V_{exp}}{V_{MCFT}}$ | $\frac{V_{exp}}{V_{ACI}}$ | $\frac{V_{exp}}{V_{EC2-03}}$ |
|---------|-----------------------------|----------------------------|---------------------------|------------------------------|
| Average | 1.24                        | 1.14                       | 1.27                      | 1.59                         |
| CoV     | 0.24                        | 0.18                       | 0.20                      | 0.43                         |
| Minimum | 0.69                        | 0.84                       | 0.70                      | 0.70                         |
| Maximum | 1.89                        | 1.62                       | 1.79                      | 2.65                         |

Note: CoV = coefficient of variation.

ACI 318 (2008), and EC2-03 (2003) are summarized in Table 3. The mean ratio of the experimental to predicted strength and its coefficient of variation are 1.24 and 0.24, 1.14 and 0.18, 1.27 and 0.20, and 1.59 and 0.43 for the proposed model, MCFT (Bentz *et al.* 2000), ACI 318 (2008), and EC2-03 (2003), respectively. Comparison of available models with experimental data indicates that MCFT (Bentz *et al.* 2000) and the proposed model produce better mean ratio of the experimental to predicted strength than the ACI 318 (2008) model and EC2-03 (2003). The truss model of EC2-03 (2003) does not incorporate the concrete contribution. This leads to very conservative results when compared with experimental tests of shear-critical reinforced concrete beams.

To investigate the validity and applicability of the proposed model across the range of several key parameters including compressive strength of concrete, aspect ratio, and transverse reinforcement ratio; the ratio of experimental shear strength to shear strength calculated from the proposed model versus compressive strength of concrete  $f'_c$ , aspect ratio  $a/d$ , and transverse reinforcement ratio  $\rho_w$  are plot in Fig. 12. The good correlation between the experimental and predicted strengths across the range of compressive strength of concrete, aspect ratio, and transverse reinforcement ratio indicates that the proposed model well represents the effects of these key parameters.

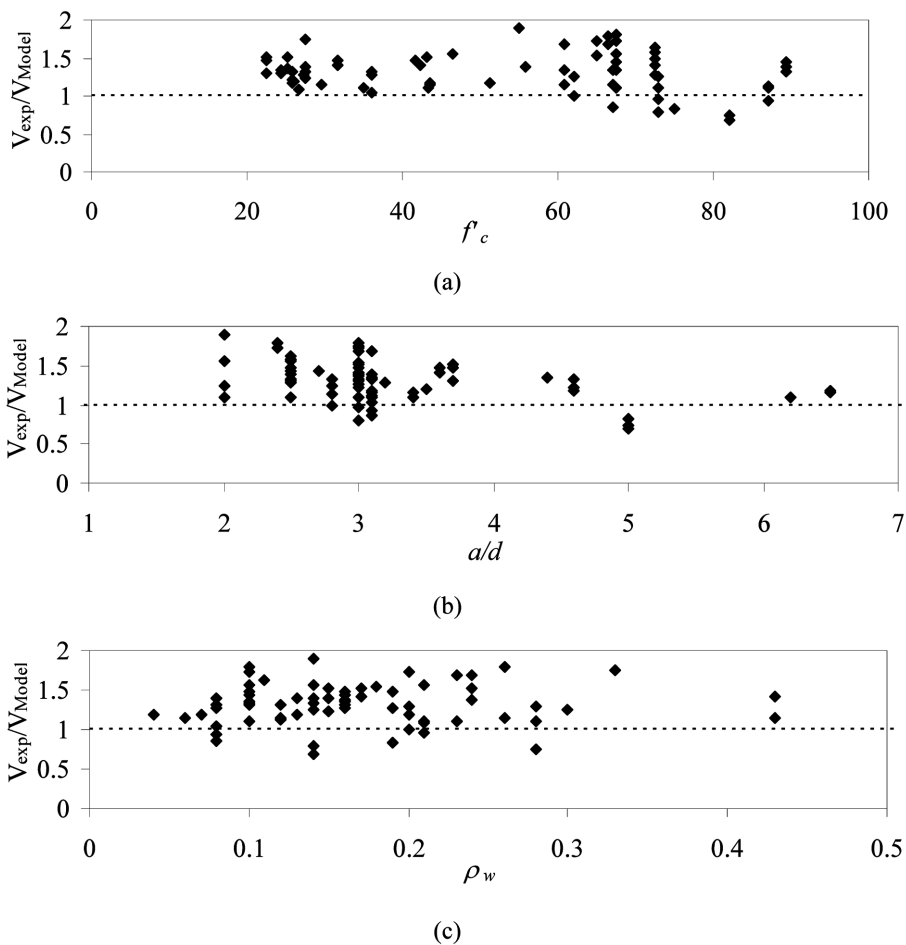


Fig. 12 Variation of experimental to predicted strength ratio as a function of key parameters

## 6. Conclusions

In this paper, a theoretical method to compute the inclination of struts and predict the shear strength of RC beams is proposed. The predicted developments of inclinations of compression struts along the shear span of the RC beams agreed fairly well with the experimental results. There is also good correlation between the shear strengths obtained and the published experimental data with the average ratio of experimental to predicted shear strength of the 71 RC beams being 1.24. This proposed method provides a useful tool for obtaining the shear strength of RC beams.

## References

- ACI-ASCE Committee 445 (1998), "Recent approaches to shear design of structural concrete", *J. Struct. Eng.-ASCE*, **24**(12), 1375-1417.
- ACI Committee 318 (2008), "Building code requirements for structural concrete and commentary", American Concrete Institute, Farmington Hills.
- AASHTO (2004), "Standard Specification for Highway Bridges".
- Al-Nahlawi, K.A. and Wight, J.K. (1992), "Beam analysis using concrete tensile strength in truss model", *ACI Struct. J.*, **89**(3), 284-289.
- Al-Nahlawi, M.K.A. (1989), "An experimental and analytical study of shear strength of lightly reinforced concrete beams", Ph.D. Thesis, University of Michigan.
- Bentz, E.C. (2000), "Sectional analysis of reinforced concrete members", Ph.D. Thesis, Department of Civil Engineering, University of Toronto.
- Bhide, S.B. and Collins, M.P. (1989), "Influence of axial tension on the shear capacity of reinforced concrete members", *ACI Struct. J.*, **86**(5), 570-581.
- Bresler, B. and Scordelis, A.C. (1963), "Shear strength of reinforced concrete beams", *ACI J.*, **60**(1), 51-72.
- CEP-FIP (1978), *Model Code for Concrete Structures*, 3<sup>rd</sup> Edition, Comite-Euro-International du Beton/Federation Internationale de la Precontrainte, Paris.
- CSA-A23.3-04 (2004), "Design of concrete structures", Canadian Standards Association.
- Cladera, A. and Mari, A.R. (2005), "Experimental study on high-strength concrete beams failing in shear", *Eng. Struct.*, **27**(10), 1519-1527.
- Collins, M.P. and Mitchell, D. (1991), *Prestressed Concrete Structures*, Prentice Hall, Englewood Cliffs, N. J., USA.
- Dilger, W. (1966), "Veränderlichkeit der Biege- und Schubsteifigkeit bei Stahlbetontragwerken und ihr Einflub auf Schnittkraftverteilung und Traglast bei statisch undestimmter Lagerung", Deutscher Ausschuss für Stahlbeton, Heft 179, Berline, Germany.
- European Committee for Standardization, prEN 1992-1-1:2003, Eurocode 2 (2003), "Design of concrete structures, Part 1: General rules and rules for buildings", Revised final draft, Brussels, Belgium.
- Karayannis, C.G. and Chalioris, C.E. (1999), "Experimental investigation of the influence of stirrups on the shear failure mechanism of reinforced concrete beams", *Proceedings of the 13th Hellenic Conference on Concrete*, Rethymnon, Greece, **1**, 133-141.
- Johnson, M.K. and Ramirez, J.A. (1989), "Minimum shear reinforcement in beams with high strength concrete", *ACI Struct. J.*, **86**(4), 376-382.
- Kim, J.H. and Mander, J.B. (1999), "Truss modeling of reinforced concrete shear-flexure behavior", MCEER-99-0005, The State University of New York at Buffalo.
- Kong, P.Y.L. and Rangan, B.V. (1998), "Shear strength of high-performance concrete beams", *ACI Struct. J.*, **95**(6), 677-687.
- Morsch, E. (1902), "Der Eisenbetonbau seine Theorie und Anwendung (Theory and Applications of Reinforced Concrete)", Verlag Konrad Wittwer, Stuttgart.
- Li, B. and Tran, C.T.N. (2008), "Reinforced concrete beam analysis supplementing concrete contribution in truss

- models”, *Eng. Struct.*, **30**(11), 3285-3294.
- Narayanan, R. and Darwish, I.Y.S. (1988), “Use of steel fibers as shear reinforcement”, *ACI Struct. J.*, **84**(3), 216-227.
- Ozcebe, G., Ersoy, U. and Tankut, T. (1999), “Evaluation of minimum shear reinforcement requirements for higher strength concrete”, *ACI Struct. J.*, **96**(3), 361-369.
- Placas, A. and Regan, P.E. (2003), “Shear failure of reinforced concrete beams”, *ACI Struct. J.*, **100**(2), 763-773.
- Priestley, M.J.N., Verma, R. and Xiao, Y. (1994), “Seismic shear strength of reinforced concrete columns”, *J. Struct. Eng.-ASCE*, **120**(8), 2310-2329.
- Rahal, K.N. and Al-Shaleh, K.S. (2004), “Minimum transverse reinforcement in 65 MPa concrete beams”, *ACI Struct. J.*, **101**(6), 872-878.
- Rahal, K.N. (2006), “Shear behavior of reinforced concrete beams with variable thickness of concrete side cover”, *ACI Struct. J.*, **103**(2), 171-177.
- Ramirez, J.A. and Breen, J.E. (1991), “Evaluation of a modified truss-model approach for beams in shear”, *ACI Struct. J.*, **88**(5), 562-571.
- Regan, P.E. (1969), “Shear in reinforced concrete beams”, *Mag. Concrete Res.*, **21**(66), 31-42.
- Ritter, W. (1899), “Die Bauweise hennebique”, *Schweizerische Bauzeitung*, Zurich, Switzerland.
- Rudra, P. (2006), *Getting Started with MATLAB 7: A Quick Introduction for Scientists and Engineers*, Oxford University Press.
- Tompos, E.J. and Frosch, R.J. (2002), “Influence of beam size, longitudinal reinforcement, and stirrup effectiveness on concrete shear strength”, *ACI Struct. J.*, **99**(5), 559-567.
- Vecchio, F.J. and Collins, M.P. (1986), “The modified compression-field theory for reinforced concrete elements subjected to shear”, *ACI J.*, **83**(2), 219-231.
- Vecchio, F.J. and Shim, W. (2004), “Experimental and analytical reexamination of classic concrete beam tests”, *J. Struct. Eng.-ASCE*, **130**(3), 460-469.
- Walraven, J.C. (1981), “Fundamental analysis of aggregate interlock”, *J. Struct. Div.*, **107**(11), 2245-2270.
- Wong, S.H.F. and Kuang, J.S. (2011), “Predicting shear strength of RC exterior beam-column joints by modified rotating-Angle softened-Truss Model”, *Comput. Concrete*, **8**(1), 59-70.
- Yoon, S.Y., Cook, W.D. and Mitchell, D. (1996), “Minimum shear reinforcement in normal, medium, and high strength concrete beams”, *ACI Struct. J.*, **93**(5), 1-9.